Auton Robot (2007) 23: 275–292
DOI 10.1007/s10514-007-9047-6

Environment adaptation of a new staircase-climbing wheelchair

R. Morales · A. Gonzalez · V. Feliu · P. Pintado

Received: 24 February 2006 / Accepted: 10 July 2007 / Published online: 15 August 2007

Abstract This paper describes the mechanical devices conforming a novel wheelchair prototype capable of climbing staircases. The key feature of the mechanical design is the use of two decoupled mechanisms in each axle, one to negotiate steps, and the other to position the axle with respect to the chair to accommodate the overall slope. This design simplifies the control task substantially. Kinematic models are necessary to describe the behavior of the system and to control the actuated degrees of freedom of the wheelchair to ensure the passenger's comfort. The choice of a good climbing strategy simplifies the control and decreases the power consumption of the wheelchair. In particular, we demonstrate that if the movement of the wheelchair has the same slope as the racks or the same slope as the terrain that supports the wheel axles (depending on the configuration mechanism), control is easier and power consumption is less. Experimental results are reported which show the behavior of the prototype as it moves over different situations: (a) ascending a single step of different heights using different climbing strategies; and (b) climbing a staircase using an appropriate climbing strategy that simplifies the control and reduces the power consumption of the wheelchair.

Keywords Wheelchair · Stair climbing · Kinematic model · Trajectory generation · Environment adaptation

R. Morales (✉) · A. Gonzalez · V. Feliu · P. Pintado
School of Industrial Engineering, University of Castilla-La Mancha, 13071 Ciudad Real, Spain
e-mail: Rafael.Morales@uclm.es

1 Introduction

Since wheelchairs first appeared, there have only been minor changes in their basic design. One important development was that of electric-powered wheelchairs because they provide functional mobility for people with both lower and upper extremity impairments (Jones and Sanford 1996; Woods and Watson 2003). The advent of single-board microprocessors in the mid-1970s allowed controllers to be improved to enhance drivability and safety (Attali and Pelisse 2001; Miller and Slack 1995). Nevertheless, architectural barriers still exist in many cities and buildings, and it is expensive and time consuming, if not impossible, to eliminate all of them. Since a standard wheelchair becomes a useless device when faced with such barriers, there have been a number of designs for wheelchairs capable of negotiating architectural barriers. The first commercial models were based on a single-section track mechanism, and became available in the mid 1990s (Sunwa CO. Ltd.). Some disadvantages of these tracked systems are that the entire track is forced to rotate on the edge of the first step when initiating descent (a difficult and dangerous operation), and low locomotion efficiency in barrier-free environments for which wheels are the best solution to attain high efficiency. The problem with these systems arises when there appear architectural barriers. The wheels must then be helped to overcome obstacles. A commonly used solution is to group two, three, or four wheels in a rolling cluster. The simplest models are small platforms to carry light wheelchairs (www.thewheelchairlift.co.uk). A negative aspect of this solution is the need for an assistant. To operate the system without assistants, a new solution is based on several wheels arranged in a rotating link (clusters). There are, for example, mechanisms that use a single rotating link

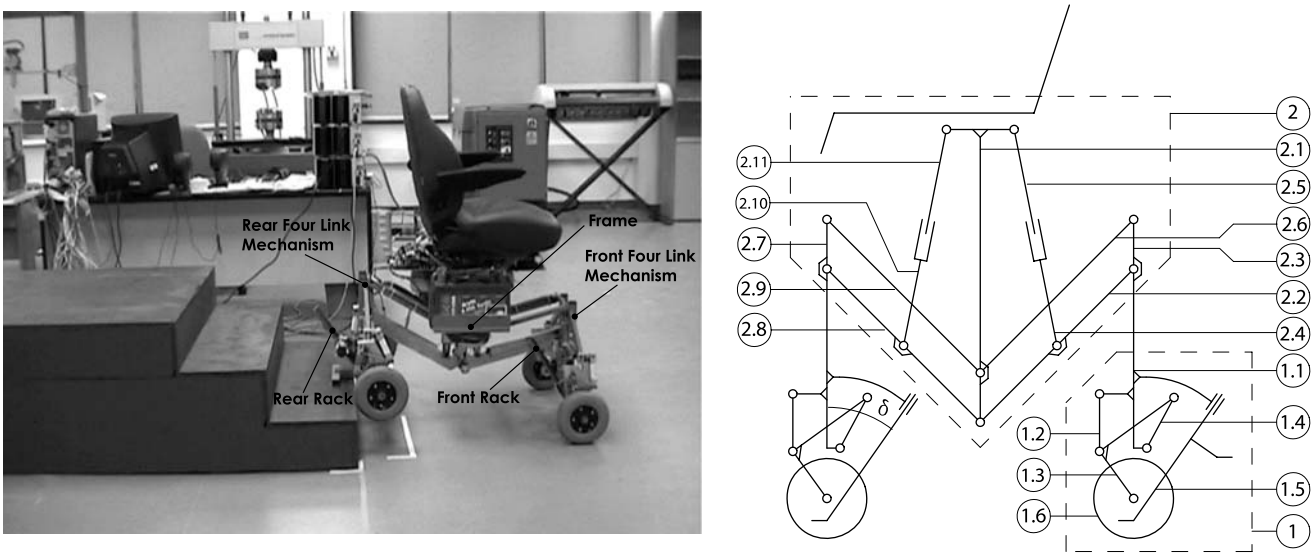

Fig. 1 **A** Design prototype. **B** Prototype scheme

(Kamen et al. 2002; Ding et al. 2004). While the mechanical design is quite simple, the chair is very sophisticated since it relies on dynamic control to maintain an upright position. There are motion phases during climbing or descending when the chair is standing on just two wheels with a common axis. The major drawback of this design is the very high cost of meeting reasonable safety standards. There are alternative designs which use several rotating links (Lawn and Ishimatzu 2003). These mechanisms have good rolling efficiency and conceptual simplicity but present a high actuating cluster torque, a large number of wheels that have to be driven and braked, difficulty in adding a steering mechanism, and a dramatic increase in weight, size, and cost.

Legs are a good method of locomotion in highly unstructured environments (Hirose 1984; Altendofer and Moore 2001), but have low efficiency in barrier-free environments. The best way to solve the problem is to use hybrid systems. These devices combine legs (high terrain adaptability) with wheels (high efficiency and payload capability). There are two ways to exploit this synergy: the first includes articulated-wheeled robots with the wheel attached to the end of the leg. Most of these systems have several types of locomotion: rolling mode, where the systems act like a conventional wheeled vehicle; walking mode, where the wheels are blocked and the vehicles act as legged systems; and a hybrid mode using both legs and wheels (Grand et al. 2004; Hirose and Takeuchi 1996). Some have been designed with the objective of providing mobility for disabled people (Wiesspeiner and Windischbacher 1995). A negative point is that the very many degrees of freedom require greater energy consumption and prototype mass. The second kind of hybrid systems consists of robots with independent legs and wheels that operate in coordination. These vehicles are simpler and lighter, and only use the hybrid mode of locomotion (Guccione and Muscato 2003). Some have been developed to help disabled people (Wellman et al. 1995). A drawback is the major variation in the inclination angle of the chair during the step-climbing process.

The wheelchair prototype proposed in this paper (Fig. 1A) maintains the behavior of commercial powered wheelchairs but with the additional properties of: (a) a capability of adapting to the environment overcoming special profiles characterized by obstacles with vertical slopes (discontinuities); (b) a capability of moving the system, in a comfortable way for the passenger, over continuous smooth profiles; and (c) a capability of ascending or descending staircases. It is very important to note that these new qualities are attained without the necessity of personal assistance. Moreover, its additional degrees of freedom allow different climbing strategies while maintaining verticality (Morales et al. 2006a).

The paper is organized as follows: A description of the mechanical design is proposed in Sect. 2. Section 3 explains how the election of an appropriate movement strategy allows the ascent or descent of staircases while maintaining passenger comfort, simplifies the control tasks, and reduces power consumption. The control system is described in Sect. 4, and illustrative experimental results are presented in Sect. 5. Finally, some concluding remarks and suggested ideas for future research are presented in Sect. 6.

2 Mechanical system

Most of the prototypes presented in the previous sections share the common problems of complexity, heaviness, and

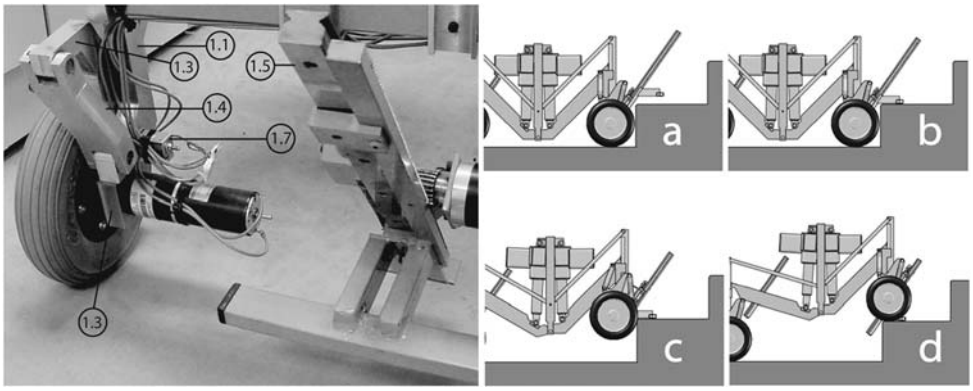

Fig. 2 **A** Details of climbing mechanism. **B** Sequence of step ascent

lack of flexibility when presented with different obstacles. These disadvantages can be solved when the staircase climbing process is split into two different problems, using a distinct mechanical device for each: (a) climbing a single step of variable height; (b) providing stability for the entire mechanism while the wheelchair is on the stair. The system designed to solve the first problem is denoted the *climbing mechanism* and the other the *positioning mechanism*. Figure 1B shows the scheme of the whole system. The parts of the climbing mechanism are numbered 1.X and the elements of the positioning mechanism are numbered 2.X (see Figs. 1B and 2A). The use of two decoupled mechanisms provides additional advantages such as simplification of the computer simulations, an easier way to develop revisions in the mechanical devices, and faster development of the mechanical components. Due to the low efficiency of other mechanisms, this system uses wheels for locomotion. Moreover, we can claim that, during the movement of the mechanism on the stair, the system remains at all times in stable equilibrium. This is a very important aspect to ensure safety. Other features are: reliability, high payload capability, light weight, control simplicity, low cost, and ease of manufacture.

2.1 Climbing mechanism

The climbing mechanism (see Figs. 1B and 2A) is the device that allows the wheelchair to surmount a single step. The system has two such mechanisms—one front and one rear. When the climbing mechanism reaches a step, a rack (1.5) is deployed which allows the wheelchair to climb the step. The support is connected to the chassis with a prismatic joint at a fixed angle (δ). A four-link mechanism is added (1.1, 1.2, 1.3, and 1.4) which allows the wheel to move backwards to avoid interference with the step. This new degree of freedom can be canceled with an electromagnetic lock (1.7). The maximum step height that the wheelchair can surmount is 215 mm. Figure 2B shows the sequence of a step ascension. When the system faces a step the rack is deployed. When this touches the top of the step, the electromechanical solenoids jamming the four-link mechanism are unlocked, and the weight is at once transferred from the rear wheel to the rear rack. The wheel can now move backwards to surpass the step. The mechanism of the rear wheel is now free to move, making it possible to surmount the step. When this has taken place, the wheel moves back to its original position, triggering retraction of the rack. This process is carried out until the wheelchair mechanism has completely surmounted the step. The weight is now transferred to the rear wheel until the wheel bar has again locked. Finally, the process ends with the rear rack withdrawing to its original position. The system is now ready to climb another step.

2.2 Positioning mechanism

The positioning mechanism is the system that ensures the verticality of the wheelchair and positions the front and rear climbing mechanisms to accommodate the overall slope. The system requirements are: compact design, reliability, high payload capability, light weight, and low cost. To attempt to satisfy these requirements, we think that the best choice is a parallel mechanism. The one that we propose is a closed-loop mechanism in which the mobile platform is connected to the base by at least two serial kinematic chains. The first applications of these closed loop robots were to tire-testing machines (Gough and Whitehall 1962) and in the motion platform for pilot training simulators (Stewart 1965). The main advantage of this scheme is its high stiffness and load capacity, of great importance for carrying heavier patients (Cooper et al. 1999). Our prototype presents a weight-payload ratio that is superior to other climbing wheelchairs and climbing robots (Gonzalez et al. 2007). The disadvantages are that the complicated structure of these mechanisms limits the motion of the platform, and the workspace is more complex. Figure 1B shows the parts of the positioning mechanism. The chair seat is joined to parts 2.1 and 2.3. The parts 2.6 are the mobile platforms to which the climbing mechanisms are attached. The movements of the mobile platforms are driven by the two linear actuators 2.5,

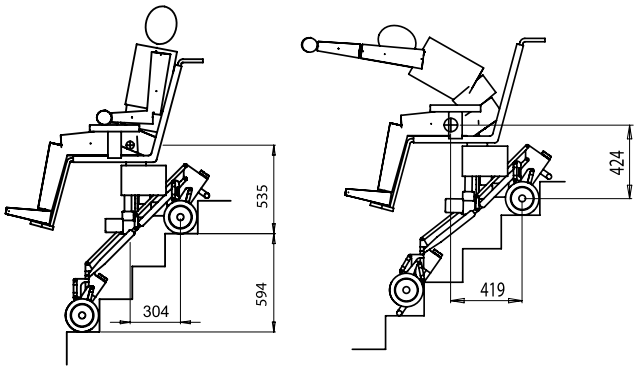

Fig. 3 Centre of mass of the entire system (human and wheelchair): **A** standard position; **B** human body is inclined

2.4. The basic tasks that the positioning mechanism performs in the staircase climbing process are: ensuring horizontality while the first climbing mechanism operates on the first steps with the second climbing mechanism still away from the staircase; accommodating the wheel base to a multiple of the step width; simultaneous step negotiating of both climbing mechanisms; and negotiating the last steps by the second climbing mechanism when the first has reached the top of the staircase. The second task of the positioning system is important to ensure comfortable ascent and descent of a staircase. The synthesis of the positioning mechanisms is designed to ensure that the accommodating process for all staircases is constructed in conformity with Norma Din 18065.

2.3 Mechanical stability

The system is always in stable equilibrium. The weight is transferred at all times to horizontal surfaces, making it unnecessary to rely on friction to ensure safety, and the support polygon (contact points between the vehicle and the flat surface) is always greater than or equal to the support polygon of conventional powered wheelchairs. We assume that since the climbing/descending process is a delicate task the user will not make abrupt movements that could cause instability of the system. We carried out some simulations to check the stability of the system when the wheelchair is ascending or descending staircases. The staircase used in the simulations is the most unfavorable case allowed by Norma Din 18065 (215 mm). Since a human model was needed, we made an android model according to (Hanavan 1964; Kwon 2001) with simple geometrical elements obtained by means of various anthropometric measurements of the human body. In particular, we used the model of a 25-year-old and 82.5 kg weight man. Figure 3 illustrates the position of the centre of mass of the system (human and wheelchair) on the staircase when the passenger is in a normal position and in an inclined position. The stability of the entire system is guaranteed in both cases.

3 Climbing strategies

The kinematic model presented in Morales et al. (2006b) allows full motion of the degrees of freedom of the whole system, and can be adapted to a continuous smooth profile or a profile consisting of flat floor and staircase. The inverse kinematic model makes it possible to determine the real time trajectories for the articulated degrees of freedom of the wheelchair. This is important since comfortable motion of the wheelchair requires the motion of all the degrees of freedom in order to maintain the desired motion of the system as a whole. The choice of a good strategy of motion will mean that the wheelchair will be able to move on a continuous smooth profiles or climb stairs using its additional degrees of freedom. In this section, we describe the strategies of movement of the wheelchair as it moves on these profiles, but emphasize the climbing motion because the configuration of the mechanism (and the kinematic model) must change as the stair is navigated. This situation involves good synchronization and precise coordinate motion of all the degrees of freedom (actuators). The importance of selecting a particular climbing strategy is because it influences the verticality of the chair frame, the comfortable trajectory of the passenger (the wheelchair will usually carry a handicapped or injured person), and the power consumption. In the following, we shall demonstrate, in all the possible configurations, that the choice of an appropriate movement strategy allows staircases to be climbed or descended while maintaining passenger comfort. The verticality of the chair is also maintained. This is done by moving only a subset of all the degrees of freedom available in the wheelchair (the rest of the actuated degrees of freedom are kept constant), thereby decreasing the power consumption.

3.1 Trajectory of the chair frame of the wheelchair with the same slope as the rear or the front axle

In this configuration the wheelchair is supported on four wheels (see Fig. 4A). The rear and front axles are rolling on terrains with different slopes (α_1 and α_2), and the angles μ_i are defined to find the geometrical connection between the vectors which comprise the general kinematic scheme. The initial expressions that define the current position of the wheelchair were explained in Morales et al. (2006b), and are the following:

$$\mathbf{P}_g = \mathbf{f}(\theta_3) + l_6 e^{j(\gamma+\frac{\pi}{2}+\mu_6)} + l_4 e^{j(\gamma+\frac{3\pi}{2}-\theta_2)} + l_5 e^{j(\gamma+\frac{\pi}{2}+\mu_5)}, \quad (1)$$

$$\mathbf{P}_g = \mathbf{f}(\theta_4) + l_1 e^{j(\gamma+\frac{\pi}{2}+\mu_5)} - l_3 e^{j(\gamma+\frac{\pi}{2}+\theta_1)} + l_5 e^{j(\gamma+\frac{\pi}{2}+\mu_5)}. \quad (2)$$

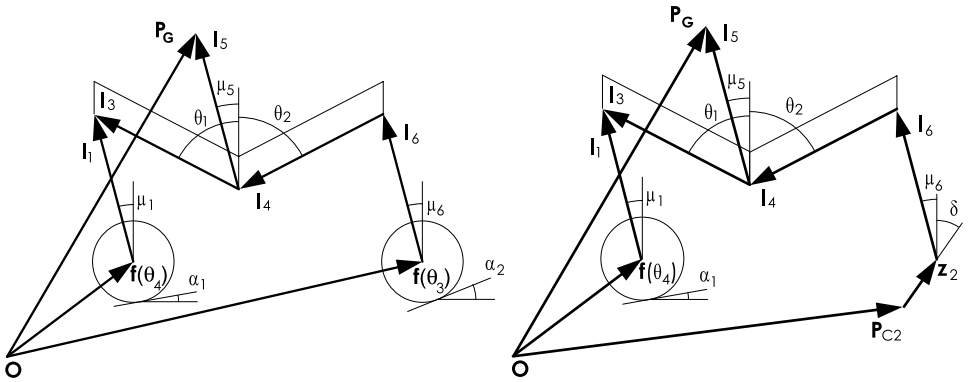

Fig. 4 General kinematic scheme when the wheelchair is supported: **A** on four wheels; **B** on rear rack and front wheels

If the mechanism performs an incremental movement from this current position, the new situation can be expressed as follows:

$$\begin{aligned}\mathbf{P}_g + \Delta\mathbf{P}_g = {} & \mathbf{f}(\theta_3) + \Delta\mathbf{f}(\theta_3) + l_6 e^{j(\gamma+\frac{\pi}{2}+\mu_6)} e^{j\Delta\gamma} \\ & + l_4 e^{j(\gamma+\frac{3\pi}{2}-\theta_2)} e^{j(\Delta\gamma-\Delta\theta_2)} \\ & + l_5 e^{j(\gamma+\frac{\pi}{2}+\mu_5)} e^{j\Delta\gamma}, \end{aligned} \tag{3}$$

$$\begin{aligned}\mathbf{P}_g + \Delta\mathbf{P}_g = {} & \mathbf{f}(\theta_4) + \Delta\mathbf{f}(\theta_4) + l_1 e^{j(\gamma+\frac{\pi}{2}+\mu_5)} e^{j\Delta\gamma} \\ & - l_3 e^{j(\gamma+\frac{\pi}{2}+\theta_1)} e^{j(\Delta\gamma+\Delta\theta_1)} \\ & + l_5 e^{j(\gamma+\frac{\pi}{2}+\mu_5)} e^{j\Delta\gamma}. \end{aligned} \tag{4}$$

Assuming that the chair frame does not rotate ($\Delta\gamma = 0$), and that the angle of the slope trajectory has the same value as the angle of the terrain slope at the rear axle ($\Delta\mathbf{P}_g = |\Delta\mathbf{P}_g| e^{j\alpha_2}$), one has by operating on (1), (2), (3), and (4) that:

$$\Delta\theta_2 = 0, \tag{5}$$

$$|\Delta\mathbf{f}(\theta_3)| = |\Delta\mathbf{P}_g|, \tag{6}$$

$$\Delta\theta_1 = \arccos\left(\frac{|\Delta\mathbf{P}_g|\sin(\alpha_1-\alpha_2) + l_3\cos(\theta_1-\alpha_2)}{l_3}\right) - \theta_1 + \alpha_2, \tag{7}$$

$$\begin{aligned}|\Delta\mathbf{f}(\theta_4)| = {} & |\Delta\mathbf{P}_g|\cos(\alpha_1-\alpha_2) \\ & - l_3(\sin(\theta_1-\alpha_2+\Delta\theta_1) - \sin(\theta_1-\alpha_2)) \end{aligned} \tag{8}$$

which are presented in order of calculation.

Similarly, assuming that the chair frame does not rotate ($\Delta\gamma = 0$) and that the angle of the slope trajectory has the same value as the angle of the terrain slope at the front axle ($\Delta\mathbf{P}_g = |\Delta\mathbf{P}_g| e^{j\alpha_1}$), one has by operating on (1), (2), (3), and (4) that:

$$\Delta\theta_1 = 0, \tag{9}$$

$$|\Delta\mathbf{f}(\theta_4)| = |\Delta\mathbf{P}_g|, \tag{10}$$

$$\Delta\theta_2 = \arccos\left(\frac{l_4\cos(\theta_2+\alpha_2) - |\Delta\mathbf{P}_g|\sin(\alpha_1-\alpha_2)}{l_3}\right) - \theta_2 - \alpha_2, \tag{11}$$

$$\begin{aligned}|\Delta\mathbf{f}(\theta_3)| = {} & |\Delta\mathbf{P}_g|\cos(\alpha_1-\alpha_2) \\ & + l_4(\sin(\theta_2+\alpha_2+\Delta\theta_2) - \sin(\theta_2+\alpha_2)) \end{aligned} \tag{12}$$

again presented in order of calculation.

These results show that if the trajectory of the chair frame of the wheelchair moves with the same slope as the rear or front slope axle (α_1 or α_2), the entire responsibility for stabilization lies on only one of the chair frame actuators while the other is kept constant.

3.2 Trajectory of the chair frame of the wheelchair with the same slope as the rear rack or the front axle

In this configuration the wheelchair is supported on the rear rack and the front wheels (see Fig. 4B). The front axle is rolling on a terrain with slope (α_1) and the rear rack is moving with slope ($\mu = \frac{\pi}{2} - \delta$). The initial expressions that define the current position of the wheelchair were explained in Morales et al. (2006b), and are the following:

$$\begin{aligned}\mathbf{P}_g = {} & \mathbf{f}(\theta_4) + l_1 e^{j(\gamma+\frac{\pi}{2}+\mu_5)} - l_3 e^{j(\gamma+\frac{\pi}{2}+\theta_1)} \\ & + l_5 e^{j(\gamma+\frac{\pi}{2}+\mu_5)}, \end{aligned} \tag{13}$$

$$\begin{aligned}\mathbf{P}_g = {} & \mathbf{P}_{C2} + z_2 e^{j(\gamma+\frac{\pi}{2}-\delta)} + l_6 e^{j(\gamma+\frac{\pi}{2}+\mu_6)} + l_4 e^{j(\gamma+\frac{3\pi}{2}-\theta_2)} \\ & + l_5 e^{j(\gamma+\frac{\pi}{2}+\mu_5)}. \end{aligned} \tag{14}$$

If the mechanism performs an incremental movement from this current position, the new situation can be expressed as follows:

$$\begin{aligned}\mathbf{P}_g + \Delta\mathbf{P}_g = {} & \mathbf{f}(\theta_4) + \Delta\mathbf{f}(\theta_4) + l_1 e^{j(\gamma+\frac{\pi}{2}+\mu_5)} e^{j\Delta\gamma} \\ & - l_3 e^{j(\gamma+\frac{\pi}{2}+\theta_1)} e^{j(\Delta\gamma+\Delta\theta_1)} \\ & + l_5 e^{j(\gamma+\frac{\pi}{2}+\mu_5)} e^{j\Delta\gamma}, \end{aligned} \tag{15}$$

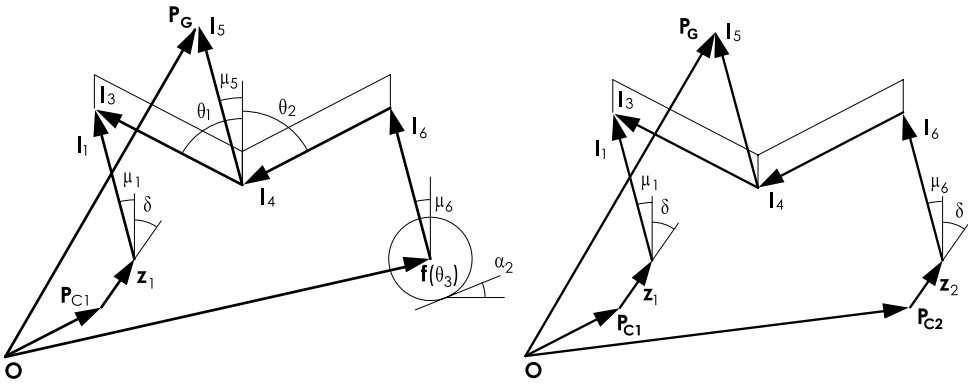

Fig. 5 General kinematic scheme when the wheelchair is supported: **A** on front rack and rear wheels; **B** on two racks

$$\begin{aligned}&\mathbf{P}_g + \Delta\mathbf{P}_g\\&= \mathbf{P}_{C2} + (z_2 + \Delta z_2)\mathrm{e}^{j(\gamma+\frac{\pi}{2}-\delta+\Delta\gamma)} + l_6\mathrm{e}^{j(\gamma+\frac{\pi}{2}+\mu_6)}\mathrm{e}^{j\Delta\gamma}\\&\quad + l_4\mathrm{e}^{j(\gamma+\frac{3\pi}{2}-\theta_2)}\mathrm{e}^{j(\Delta\gamma-\Delta\theta_2)}\\&\quad + l_5\mathrm{e}^{j(\gamma+\frac{\pi}{2}+\mu_5)}\mathrm{e}^{j\Delta\gamma}.\end{aligned} \tag{16}$$

Assuming that the chair frame does not rotate ($\Delta\gamma = 0$), and that the angle of the slope trajectory has the same value as the angle of the terrain slope at the front axle ($\Delta\mathbf{P}_g = |\Delta\mathbf{P}_g|\mathrm{e}^{j\alpha_1}$), one has by operating on (13), (14), (15), and (16) that:

$$\Delta\theta_1 = 0, \tag{17}$$

$$|\Delta\mathbf{f}(\theta_4)| = |\Delta\mathbf{P}_g|, \tag{18}$$

$$\begin{aligned}\Delta\theta_2 &= \delta - \theta_2\\&\quad - \arcsin\left(\frac{l_4\sin(\delta-\theta_2) + |\Delta\mathbf{P}_g|\cos(\delta+\alpha_1)}{l_4}\right),\end{aligned} \tag{19}$$

$$\begin{aligned}\Delta z_2 &= |\Delta\mathbf{P}_g|\sin(\delta+\alpha_1)\\&\quad + l_4(\cos(\delta-\theta_2-\Delta\theta_2) - \cos(\delta-\theta_2))\end{aligned} \tag{20}$$

presented in order of calculation. Similarly, assuming that the chair frame does not rotate ($\Delta\gamma = 0$) and that the angle of the slope trajectory has the same value as the angle of the rear rack ($\Delta\mathbf{P}_g = |\Delta\mathbf{P}_g|\mathrm{e}^{j(\frac{\pi}{2}-\delta)}$), one has by operating in (13), (14), (15), and (16) that:

$$\Delta\theta_2 = 0, \tag{21}$$

$$\Delta z_2 = |\Delta\mathbf{P}_g|, \tag{22}$$

$$\begin{aligned}\Delta\theta_1 &= \arccos\left(l_3\cos(\theta_1-\alpha_1) - \frac{|\Delta\mathbf{P}_g|\cos(\delta+\alpha_1)}{l_3}\right)\\&\quad - \theta_1 + \alpha_1,\end{aligned} \tag{23}$$

$$\begin{aligned}|\Delta\mathbf{f}(\theta_4)| &= |\Delta\mathbf{P}_g|\sin(\delta+\alpha_1)\\&\quad - l_3(\sin(\theta_1+\alpha_1+\Delta\theta_1) - \sin(\theta_1+\alpha_1))\end{aligned} \tag{24}$$

presented in order of calculation. These results show that if the trajectory of the chair frame of the wheelchair moves with the same slope as the rear rack ($\mu = \delta - \frac{\pi}{2}$) or the front slope axle (α_1), the entire responsibility for stabilization lies on only one of the chair frame actuators while the other is kept constant.

3.3 Trajectory of the chair frame of the wheelchair with the same slope as the front rack or the rear axle

In this case the wheelchair is supported on the front rack and the rear wheels (see Fig. 5A). The rear axle is rolling on a terrain with slope (α_2), and the front rack is moving with slope ($\mu = \frac{\pi}{2} - \delta$). The initial expressions that define the current position of the wheelchair were explained in Morales et al. (2006b), and are the following:

$$\begin{aligned}\mathbf{P}_g &= \mathbf{f}(\theta_3) + l_6\mathrm{e}^{j(\gamma+\frac{\pi}{2}+\mu_6)} + l_4\mathrm{e}^{j(\gamma+\frac{3\pi}{2}-\theta_2)}\\&\quad + l_5\mathrm{e}^{j(\gamma+\frac{\pi}{2}+\mu_5)},\end{aligned} \tag{25}$$

$$\begin{aligned}\mathbf{P}_g &= \mathbf{P}_{C1} + z_1\mathrm{e}^{j(\gamma+\frac{\pi}{2}-\delta)} + l_1\mathrm{e}^{j(\gamma+\frac{\pi}{2}+\mu_5)}\\&\quad - l_3\mathrm{e}^{j(\gamma+\frac{\pi}{2}+\theta_1)} + l_5\mathrm{e}^{j(\gamma+\frac{\pi}{2}+\mu_5)}.\end{aligned} \tag{26}$$

If the mechanism performs an incremental movement from this current position, the new situation can be expressed as follows:

$$\begin{aligned}\mathbf{P}_g + \Delta\mathbf{P}_g &= \mathbf{f}(\theta_3) + \Delta\mathbf{f}(\theta_3) + l_6\mathrm{e}^{j(\gamma+\frac{\pi}{2}+\mu_6)}\mathrm{e}^{j\Delta\gamma}\\&\quad + l_4\mathrm{e}^{j(\gamma+\frac{3\pi}{2}-\theta_2)}\mathrm{e}^{j(\Delta\gamma-\Delta\theta_2)}\\&\quad + l_5\mathrm{e}^{j(\gamma+\frac{\pi}{2}+\mu_5)}\mathrm{e}^{j\Delta\gamma},\end{aligned} \tag{27}$$

$$\begin{aligned}\mathbf{P}_g + \Delta\mathbf{P}_g &= \mathbf{P}_{C1} + (z_1 + \Delta z_1)\mathrm{e}^{j(\gamma+\frac{\pi}{2}-\delta+\Delta\gamma)}\\&\quad + l_1\mathrm{e}^{j(\gamma+\frac{\pi}{2}+\mu_5)}\mathrm{e}^{j\Delta\gamma}\\&\quad - l_3\mathrm{e}^{j(\gamma+\frac{\pi}{2}+\theta_1)}\mathrm{e}^{j(\Delta\gamma+\Delta\theta_1)}\\&\quad + l_5\mathrm{e}^{j(\gamma+\frac{\pi}{2}+\mu_5)}\mathrm{e}^{j\Delta\gamma}.\end{aligned} \tag{28}$$

Assuming that the chair frame does not rotate ($\Delta\gamma = 0$), and that the angle of the slope trajectory has the same value

as the angle of the terrain slope at the rear axle ($\Delta\mathbf{P}_g = |\Delta\mathbf{P}_g|e^{j\alpha_2}$), one has by operating on (25), (26), (27), and (28) that:

$$\Delta\theta_2 = 0, \tag{29}$$

$$|\Delta\mathbf{f}(\theta_3)| = |\Delta\mathbf{P}_g|, \tag{30}$$

$$\Delta\theta_1 = \arcsin\left(\frac{l_3\sin(\theta_1+\delta)+|\Delta\mathbf{P}_g|\cos(\delta+\alpha_2)}{l_3}\right) - \theta_1 - \delta, \tag{31}$$

$$\Delta z_1 = |\Delta\mathbf{P}_g|\sin(\delta+\alpha_2) + l_3(\cos(\theta_1+\delta+\Delta\theta_1)-\cos(\theta_1+\delta)) \tag{32}$$

presented in order of calculation.

Similarly, assuming that the chair frame does not rotate ($\Delta\gamma = 0$) and that the angle of the slope trajectory has the same value as the angle of the front rack ($\Delta\mathbf{P}_g = |\Delta\mathbf{P}_g|e^{j(\frac{\pi}{2}-\delta)}$), one has by operating on (25), (26), (27), and (28) that:

$$\Delta\theta_1 = 0, \tag{33}$$

$$\Delta z_1 = |\Delta\mathbf{P}_g|, \tag{34}$$

$$\Delta\theta_2 = \arccos\left(l_4\cos(\theta_2+\alpha_2) - \frac{|\Delta\mathbf{P}_g|\cos(\delta+\alpha_2)}{l_4}\right) - \theta_2 + \alpha_2, \tag{35}$$

$$|\Delta\mathbf{f}(\theta_3)| = |\Delta\mathbf{P}_g|\sin(\delta+\alpha_2) + l_4(\sin(\theta_2+\alpha_2+\Delta\theta_2)-\sin(\theta_2+\alpha_2)). \tag{36}$$

These results show that if the trajectory of the chair frame of the wheelchair moves with the same slope as the front rack ($\mu = \delta - \frac{\pi}{2}$) or the rear slope axle (α_2), the entire responsibility for stabilization lies on only one of the chair frame actuators while the other one is kept constant.

3.4 Trajectory of the chair frame of the wheelchair with the same slope as the racks

In this configuration the wheelchair is supported on two racks (see Fig. 5B). The rear and front racks are moving with the same slope ($\mu = \frac{\pi}{2} - \delta$). The initial expressions that define the current position of the wheelchair were explained in Morales et al. (2006b), and are the following:

$$\mathbf{P}_g = \mathbf{P}_{C2} + z_2e^{j(\gamma+\frac{\pi}{2}-\delta)} + l_6e^{j(\gamma+\frac{\pi}{2}+\mu_6)} + l_4e^{j(\gamma+\frac{3\pi}{2}-\theta_2)} + l_5e^{j(\gamma+\frac{\pi}{2}+\mu_5)}, \tag{37}$$

$$\mathbf{P}_g = \mathbf{P}_{C1} + z_1e^{j(\gamma+\frac{\pi}{2}-\delta)} + l_1e^{j(\gamma+\frac{\pi}{2}+\mu_5)} - l_3e^{j(\gamma+\frac{\pi}{2}+\theta_1)} + l_5e^{j(\gamma+\frac{\pi}{2}+\mu_5)}. \tag{38}$$

If the mechanism performs an incremental movement from this current position, the new situation can be expressed as follows:

$$\mathbf{P}_g + \Delta\mathbf{P}_g = \mathbf{P}_{C2} + (z_2+\Delta z_2)e^{j(\gamma+\frac{\pi}{2}-\delta+\Delta\gamma)} + l_6e^{j(\gamma+\frac{\pi}{2}+\mu_6)}e^{j\Delta\gamma} + l_4e^{j(\gamma+\frac{3\pi}{2}-\theta_2)}e^{j(\Delta\gamma-\Delta\theta_2)} + l_5e^{j(\gamma+\frac{\pi}{2}+\mu_5)}e^{j\Delta\gamma}, \tag{39}$$

$$\mathbf{P}_g + \Delta\mathbf{P}_g = \mathbf{P}_{C1} + (z_1+\Delta z_1)e^{j(\gamma+\frac{\pi}{2}-\delta+\Delta\gamma)} + l_1e^{j(\gamma+\frac{\pi}{2}+\mu_5)}e^{j\Delta\gamma} - l_3e^{j(\gamma+\frac{\pi}{2}+\theta_1)}e^{j(\Delta\gamma+\Delta\theta_1)} + l_5e^{j(\gamma+\frac{\pi}{2}+\mu_5)}e^{j\Delta\gamma}. \tag{40}$$

Assuming that the chair frame does not rotate ($\Delta\gamma = 0$), and that the angle of the slope trajectory has the same value than the slope of the racks ($\Delta\mathbf{P}_g = |\Delta\mathbf{P}_g|e^{j(\frac{\pi}{2}-\delta)}$), one has by operating on (37), (38), (39), and (40) that:

$$\Delta\theta_1 = \Delta\theta_2 = 0, \tag{41}$$

$$\Delta\mathbf{z}_1 = \Delta\mathbf{z}_2 = |\Delta\mathbf{P}_g|. \tag{42}$$

The results in this case show that the actuators of the chair frame are maintained in a constant position throughout the climbing process, while the actuators of the racks are moving with the same velocity.

4 Control system

4.1 Sensorial system

Operating the wheelchair requires a fairly complex sensorial system. Eight ultrasound sensors are needed to measure the distances between the wheels and the steps and to obtain information about the climbing/descent process. They are placed two per wheel in horizontal and vertical positions. An inclinometer is placed on the frame to measure the verticality of the chair and to detect the instant at which the climbing mechanism touches the floor when being deployed. To measure the positions of the different actuated degrees of freedom, there are four encoders—two in the rear wheels and two in the racks of the climbing mechanism—and two angle sensors on linear actuators. Finally, there are four switches (one per wheel) to indicate the end positions of the six four-bar mechanisms, and eight switches (two per linear actuator and two per rack) to indicate the maximum and minimum positions for the two joints of the chair structure for the racks.

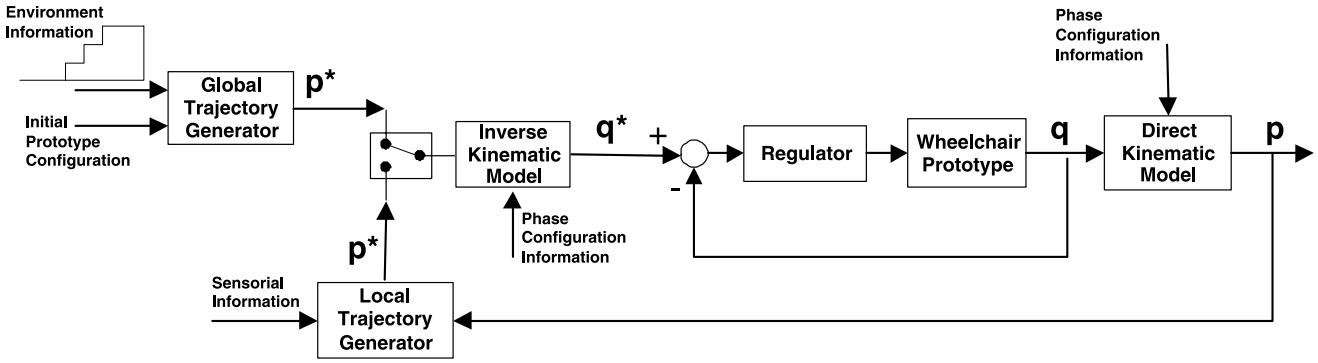

Fig. 6 Control scheme of the wheelchair prototype

4.2 Actuator system

The movement of the prototype is driven by two DC motors connected to the rear wheels, two DC motors on the front and rear racks, and two linear actuators located on the joints of the chair structure. MATRIX..3A linear power actuators were chosen for their low cost, small size, light weight, linear power and mechanico-electrical characteristics (120 W, maximum 8000 N, 5–7 mm/s, 24 V, weight 4.5 kg). These linear actuators are driven by an MD22 Advanced Motion Control PWM servo amplifier. The racks and the wheels are actuated by Maxon 148867 DC Motors with planetary gearbox (Maxon motor 203129, reduction 156:1), chosen as having the same features as the linear drives (150 W, 24 V, 8200 rpm, weight 2.2 kg). These are driven by an Advanced Motor Control EPOS 24/5 servo amplifier. Finally, four electromagnetic solenoids (one per wheel) are used to lock or unlock the mechanisms that connect the wheels to the axles.

4.3 Control scheme

Figure 6 shows the general control scheme of the wheelchair. It consists of an open-loop control term and a closed-loop control term.

4.3.1 Open-loop control term

With respect to the mechanical structure, modularity was a key factor in the design of the system. The wheelchair's driven degrees of freedom were split into two categories—the first concerning the locomotion itself (traction and step ascent), and the second concerning the posture (verticality of the chair frame). The two categories will be treated together in the control scheme. The movement of the wheelchair will be treated differently depending on the knowledge of the external environment. With perfect knowledge of the environment, a global trajectory generator is used to generate the centre of mass trajectories with the null inclination of the chair frame ($\mathbf{p}^*$). These trajectories can be constructed prior to the wheelchair starting to move. Using the inverse kinematic model presented in Morales et al. (2006b), one obtains the reference trajectories that control the angles of the motors responsible for moving the wheelchair in an open-loop fashion ($\mathbf{q}^*$). The climbing strategies described in the previous sections are implemented in the global trajectory generator. The sensorial system used in this control consists of the ultrasound sensors in the initial phase to obtain the distance between the wheelchair and the stair, and the electromagnetic solenoids that allow configuration changes.

4.3.2 Closed-loop control term

With imperfect knowledge of the environment, the information provided by the sensorial system takes on greater importance. The external and the internal sensorial systems are merged to obtain more information about the local environment of the wheelchair ($\mathbf{p}$). With these data, and the knowledge of the current configuration, the local trajectory generator develops the new trajectories of the centre of mass using a sliding mode control in the actuated degrees of freedom that control the posture, and a behavior diagram to decide the specific configuration that the wheelchair has to adopt. This local trajectory generator will not be further detailed here.

4.4 Control architecture

The control architecture is a system consisting of a main CPU, a Digital/Analog I/O board, and a serial port board. The digital output board is used to control the electromagnetic solenoids. The analog input board is used to acquire sensorial data from the different sensors. The analog output board is used to command two DC motors (the two degrees of freedom of the chair) as joint drivers based on the pulsewidth modulation technique. The serial port board is used to acquire sensorial data from the ultrasound sensors and to command four DC motors (two for the rear wheels and two for the racks) as joint drivers also based on the

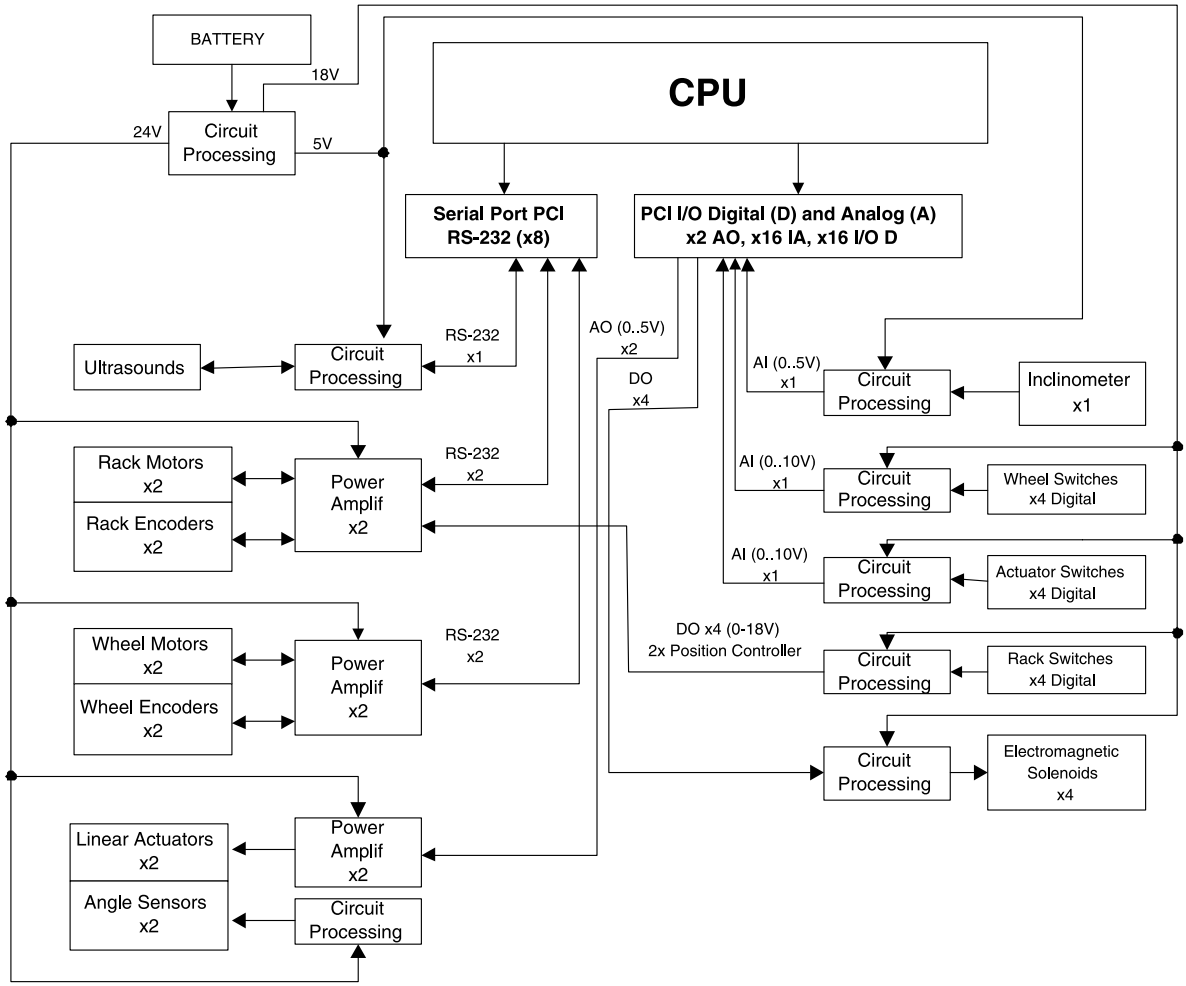

Fig. 7 Control architecture of the wheelchair

pulsewidth modulation technique. The motor positions, linear drives, and DC motors are controlled via proportional derivative (PD) control loops. The PWM servo amplifiers control the current to the motors and actuators, thus obtaining estimates of the torques at the motor shaft as long as the motors are not saturated. The system operates at 24 V nominal voltage provided by two batteries, and a conditioning circuit that provides regulated voltages at 5 V, 18 V, and 24 V. Finally, the main CPU, with the I/O and serial port boards, gathers data from the sensors and performs the computations to implement the various control schemes. The control architecture of the system is shown diagramatically in Fig. 7.

5 Experimental results

In this section, we describe the results of experiments performed to validate the climbing strategies for the wheelchair prototype. The geometrical parameters, the working environment, and some specifications of the real prototype are illustrated in Fig. 8 and their values are listed in Table 1. We studied the behavior of the prototype as it moved over different situations: (a) climbing a single step of different heights using profiles of the centre of mass with different slopes, and (b) climbing a staircase with the same slope as the rear wheels or the rear rack (depending on the configuration). In both experiments, the movements had to satisfy the following two conditions: (i) maintenance of the verticality of the seat, and the accurate tracking of the trajectory designed for the centre of mass, and (ii) the passenger's comfort in these trajectories designed for the centre of mass. This latter constraint implies that the movement of the chair frame will consist of two stages—one to accelerate the wheelchair and the other to decelerate it. Figure 9A shows the velocity profile of the centre of mass of the prototype in the experiments.

In all the experiments we calculate the stair centre of mass trajectory and we obtain the reference trajectories that control the angles of the motors in charge of moving the wheelchair in an open loop fashion. Then only the open-loop

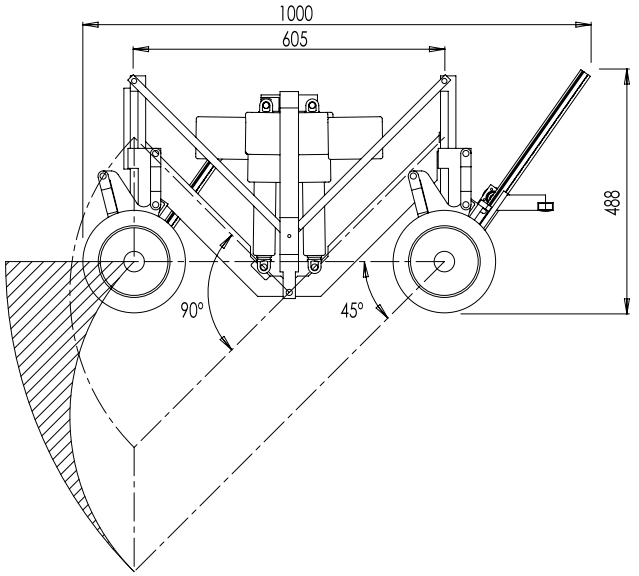

Fig. 8 Geometrical parameters and working environment (dimensions in mm)

Table 1 Some prototype specifications

Max. passenger weight	100 kg
Vehicle plus battery weight	40 kg 50 kg = 90 kg
Power source (battery)	12 V 56 Ah × 2
Operating range (time)	
Barrier free operation	6.4 h
Stair operation	3.7 h
Stair-climbing speed (max.)	3 steps per min
Speed on the flat (max.)	2 km/h
Max. height step	215 mm
Max. slope allowable	45°

control term (Sect. 4.3.1) of Fig. 6 is used. Prior to the trials, we estimated the dynamic behavior of all the actuators including their individual closed-loop controls. We found that the dynamics of these systems can be considered negligible relative to the entire chair system because the movements of the prototype as a whole are much slower than the time responses of the servo-controlled electrical motors. Data on the movement of the chair—used in the prototype and open-loop control validation—was obtained using the commercial Optotrack system. This system consists of three infrared cameras which can obtain the location and measures (6D) of several infrared markers. In our experiment, the Optotrack motion analysis system used two infrared markers to record the wheelchair trajectories. One was placed at the centre of mass of the wheelchair and the other on a horizontal surface to measure the deviation of the seat from verticality. We also used the internal hardware of the prototype to acquire data from the encoders of the wheels and the racks,

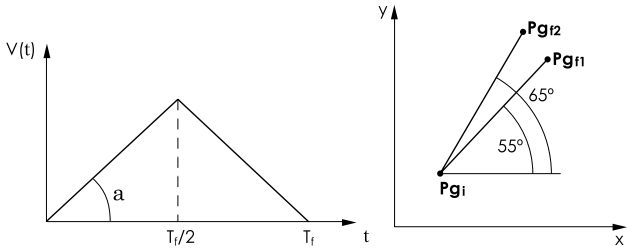

Fig. 9 **A** Profile velocity of the centre of mass in all the experiments. **B** Profile position of the centre of mass used to climb a single step

the sensors that measure the angles of the joints of the structure, and the inclination of the seat. The real-time movement of the prototype was thus appropriately recorded throughout the test. The problem of the synchronization of all the data on the prototype's movement was solved by using a trigger signal.

5.1 Climbing one step using different climbing strategies

In these two experiments, we focused on the ease of adapting the prototype to the environment when the height of the steps is variable. The experiments consisted of climbing one step of four different heights—180, 150, 120, and 90 mm—while maintaining the seat's verticality and the trajectory of the centre of mass. The two experiments were designed to illustrate that the mechanism is able to climb steps using different climbing strategies. In both experiments, the tracking trajectory of the wheelchair's centre of mass is a straight line, but with different inclination angles. The trajectory consisted of horizontal lines linked with 55° slope lines (the same slope as the racks) in the first experiment, and with 65° slope lines in the second experiment. Figure 9B shows the trajectory profiles used.

5.1.1 Experiment 1

Figures 10 and 11 show the reference and experimental trajectories of the angles of the front and rear joint (θ_1 and θ_2) when the wheelchair prototype ascends steps of different heights and the chair frame trajectory is a straight line with a slope of 55°. In Fig. 10 one observes that the distance covered by the angle of the front joint (θ_1) increases with increasing step height, and in Fig. 11 that the angle of the rear joint of the chair structure (θ_2) remains constant in all the experiments. Together, the two figures show that the responsibility for the climbing process and the maintenance of verticality of the chair is entirely supported by the linear actuator connected to the chair structure in charge of the evolution of θ_1.

Figure 12 depicts the trajectories of the front rack (z_2), and shows that the length of the rear rack increases with

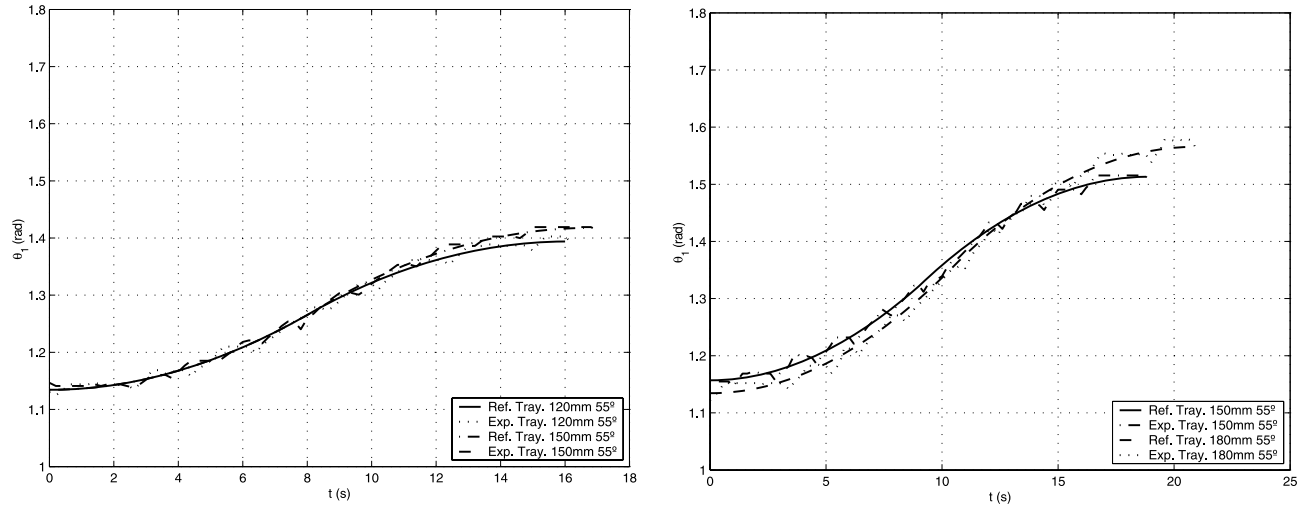

Fig. 10 Evolution of the angle of the front joint (θ_1) in the first experiment

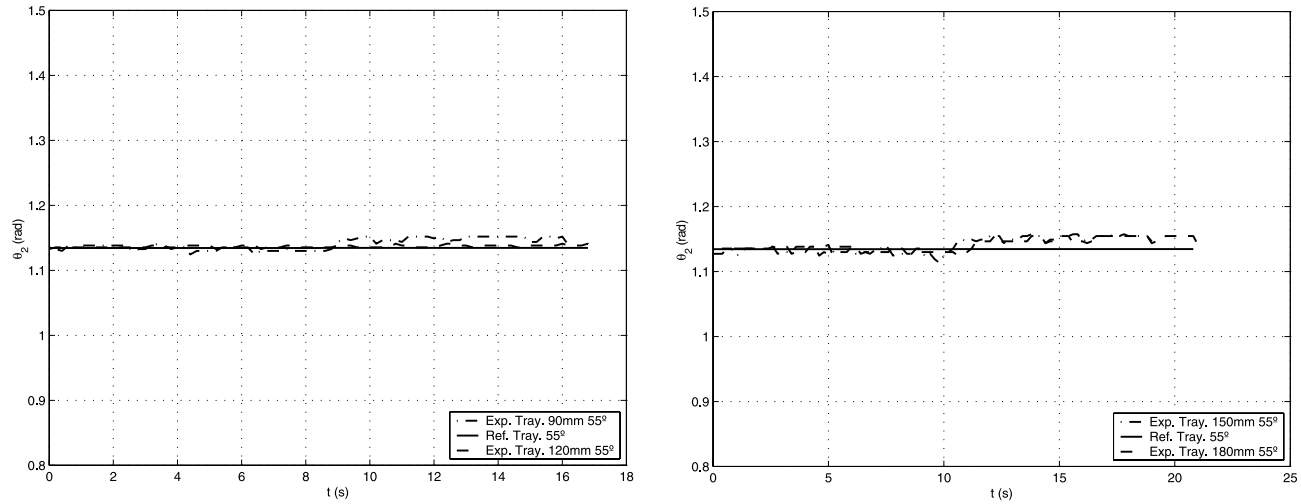

Fig. 11 Evolution of the angle of the rear joint (θ_2) in the first experiment

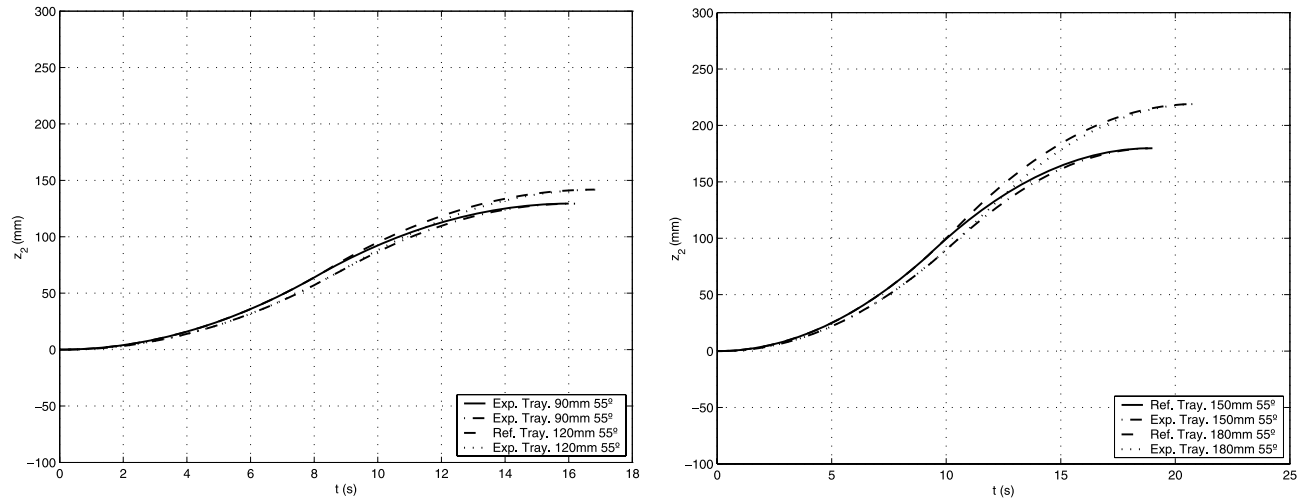

Fig. 12 Instantaneous length of the rear rack (z_2) in the first experiment

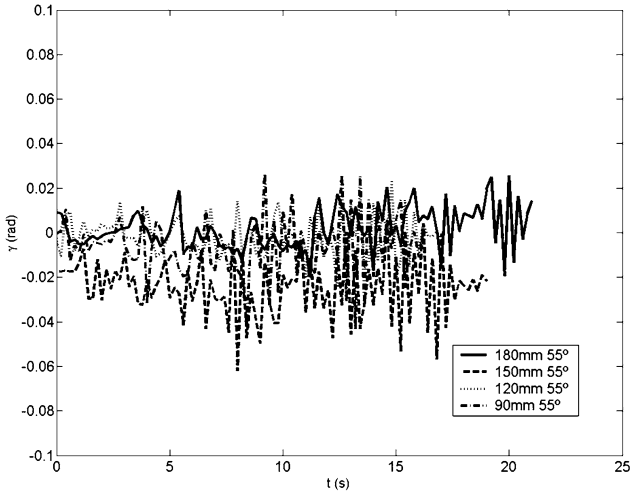

Fig. 13 Evolution of the verticality of the wheelchair (γ) in the first experiment

increasing step height. Figure 13 shows the inclination of the wheelchair (γ) in ascending different steps. In all cases, the verticality of the chair is maintained within acceptable ranges ($\pm 6°$ or ± 0.105 rad).

5.1.2 Experiment 2

Figures 14 and 15 show the reference and experimental trajectories of the angles of the front and rear joints (θ_1 and θ_2) as the wheelchair prototype ascends steps of different heights and the chair frame trajectory is a straight line with a slope of 65°. One observes that the distances covered by the angles of the front and rear joints (θ_1 and θ_2) increase with increasing step heights. In this experiment, the responsibility for the climbing process and the maintenance of verticality of the chair is supported by the two linear actuators connected to the chair structure, which are in charge of the evolution of θ_1 and θ_2.

Figure 16 depicts the trajectories of the front rack (z_2), and shows that the length of the rear rack increases when increasing step height. Figure 17 shows the inclination of the wheelchair (γ) in ascending different steps. In all cases, the verticality of the chair is maintained within acceptable ranges while climbing the different steps ($\pm 6°$ or ± 0.105 rad), but deviations from verticality are larger than in Experiment 1.

Finally Fig. 18 shows a typical example (climbing a step of 180 mm height) of an experimental spatial trajectories of the centre of mass of the wheelchair, compared with the reference trajectory.

5.2 Climbing a staircase consisting of three steps

In the experiments described in this section, we used a staircase of three steps having step dimensions 180 mm (height)

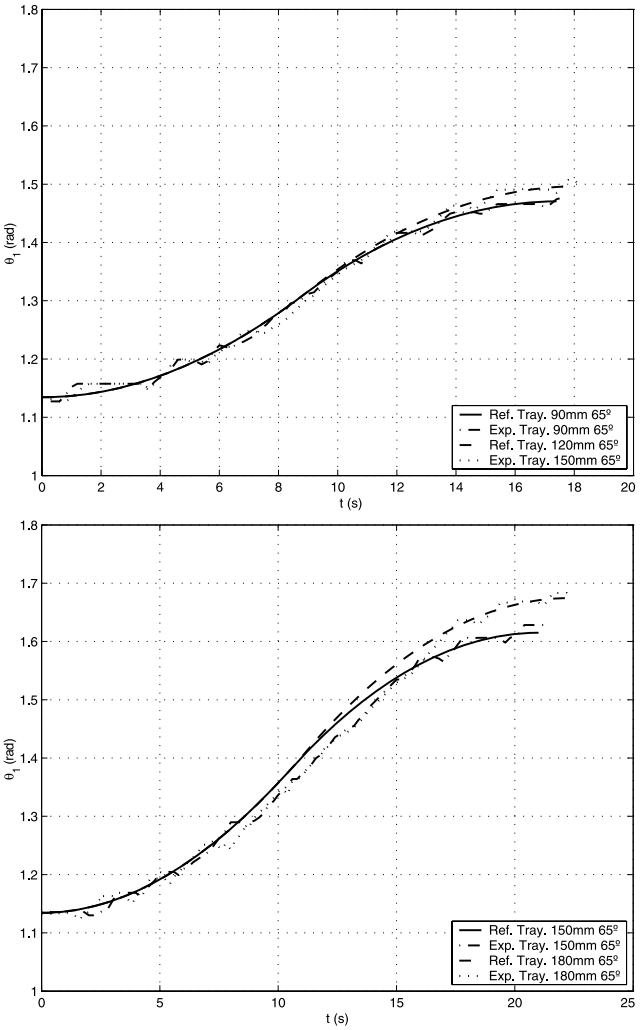

Fig. 14 Evolution of the angle of the front joint (θ_1) in the second experiment

and 300 mm (width). We used a profile consisting of straight lines with the same slope as the rear rack (when the wheelchair is in a mixed configuration or supported on the two racks) or the same slope as the rear axle (when the wheelchair is supported on two wheels) to clarify the different climbing strategies explained in Sect. 3. The trajectory thus defined must be comfortable for the passenger, meaning that inertial forces have to be small relative to gravity forces, accelerations and velocities less than the maximum comfort acceleration and velocity, and the inclination of the wheelchair null.

Figures 19A and 19B show the reference and experimental trajectories of the angles of the joints connecting the chair structure (positioning mechanism). The major deviation that appears in the middle of Fig. 19A and at the end of Fig. 21A between the reference and the experimental trajectories is due to a constraint imposed on the maximum deployment of the front linear actuator in order to protect the

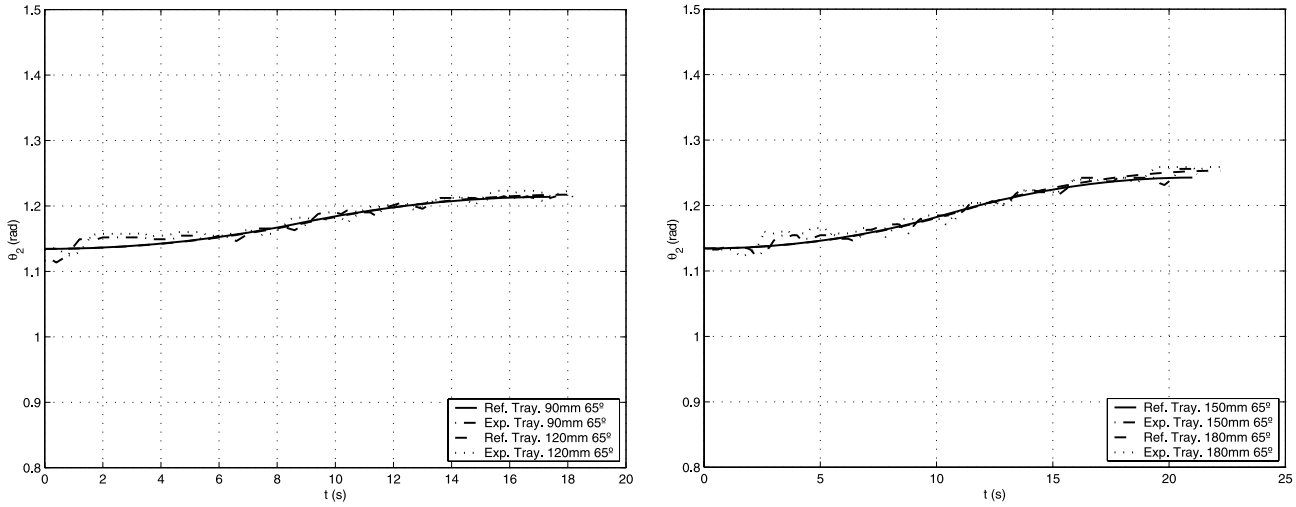

Fig. 15 Evolution of the angle of the front joint (θ_2) in the second experiment

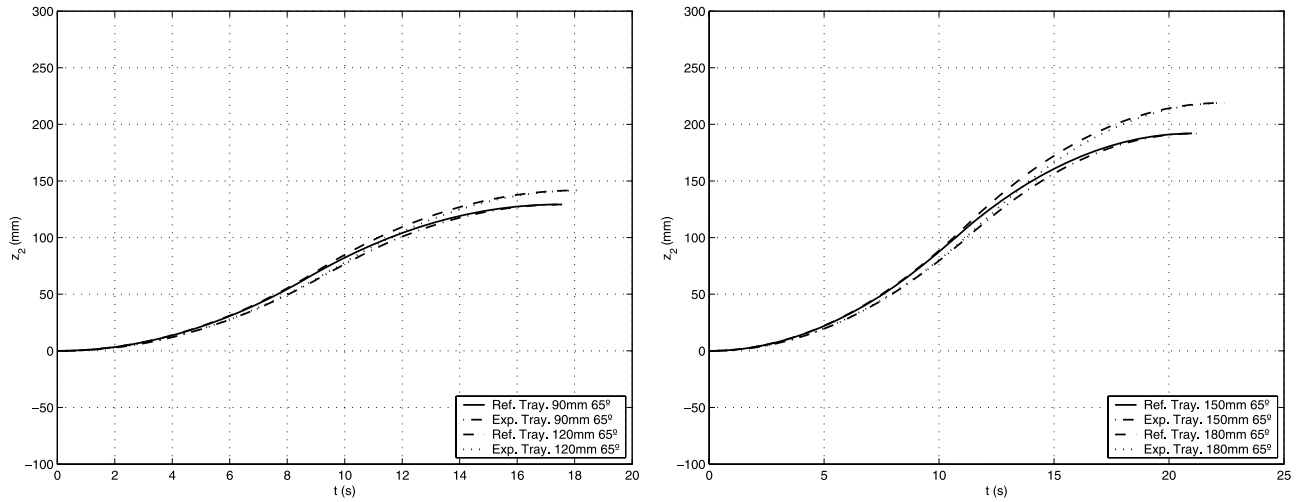

Fig. 16 Instantaneous length of the rear rack (z_2) in the second experiment

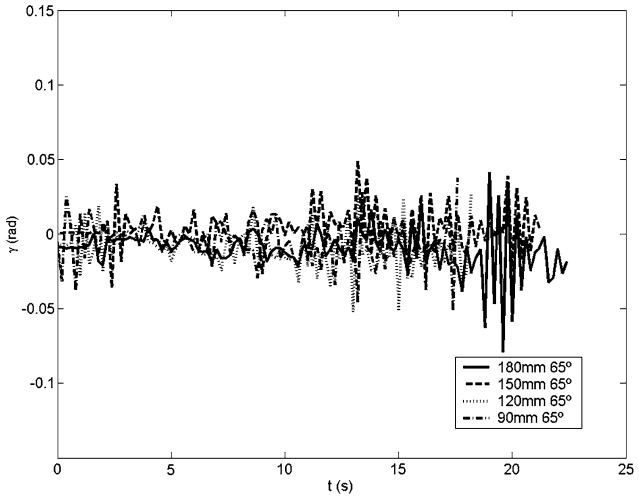

Fig. 17 Evolution of the verticality of the wheelchair (γ) in the second experiment

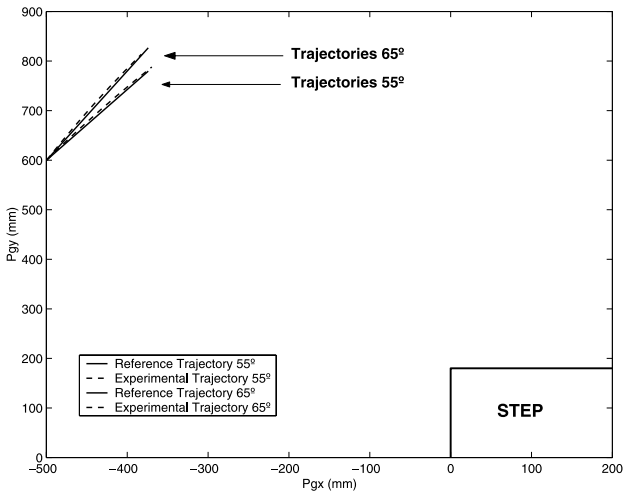

Fig. 18 Reference and experimental spatial trajectories of the centre of mass of the wheelchair while climbing a 180 mm high step

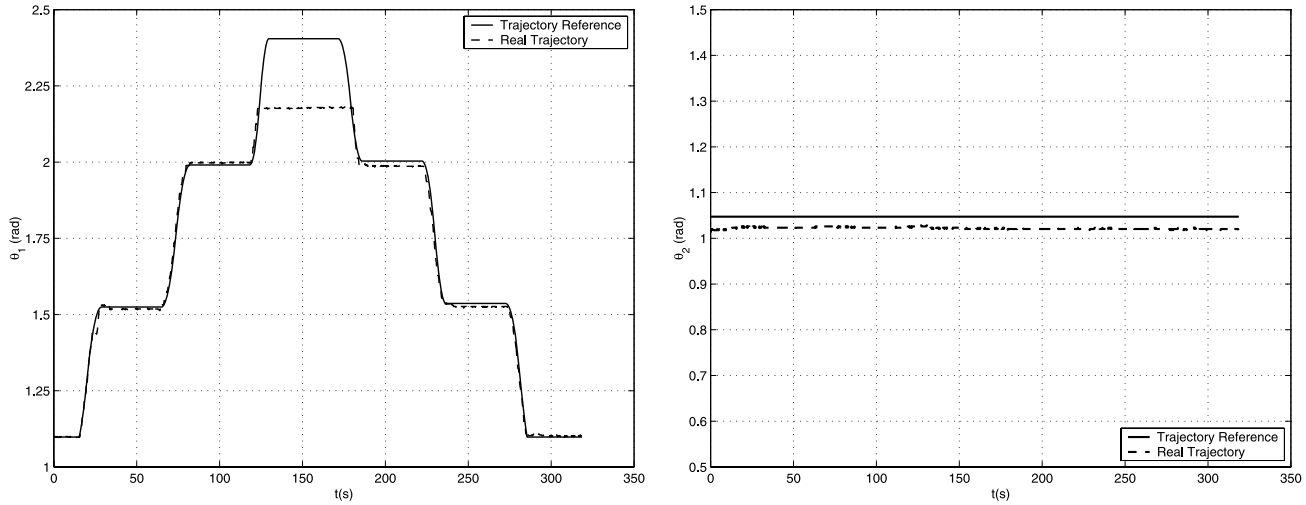

Fig. 19 **A** Evolution of the angle of the front joint (θ_1) when the prototype climbs the staircase. **B** Angle evolution of rear joint (θ_2) when the prototype climbs the staircase

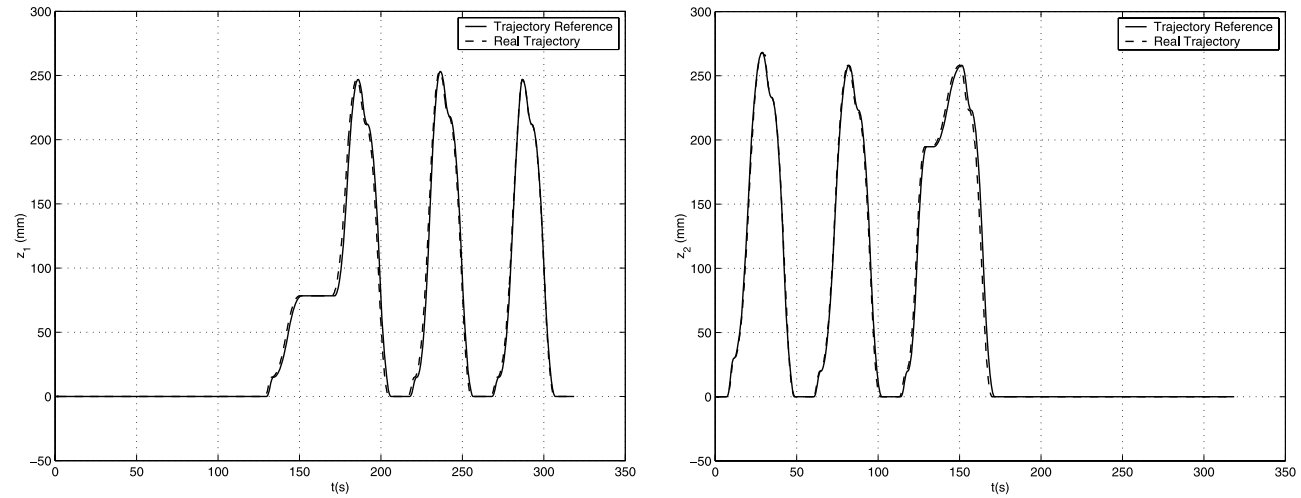

Fig. 20 **A** Position of the front rack (z_1) when the prototype climbs the staircase. **B** Position of rear rack (z_2) when the prototype climbs the staircase

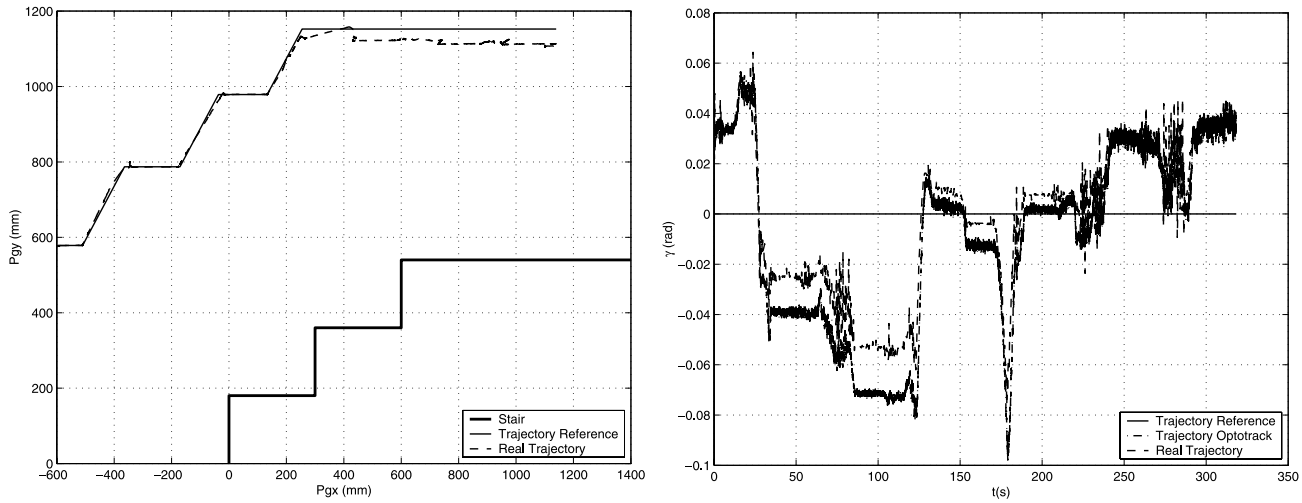

Fig. 21 **A** Trajectory of the centre of mass ($\mathbf{P}_g$) and **B** wheelchair inclination (γ) when the prototype climbs the staircase

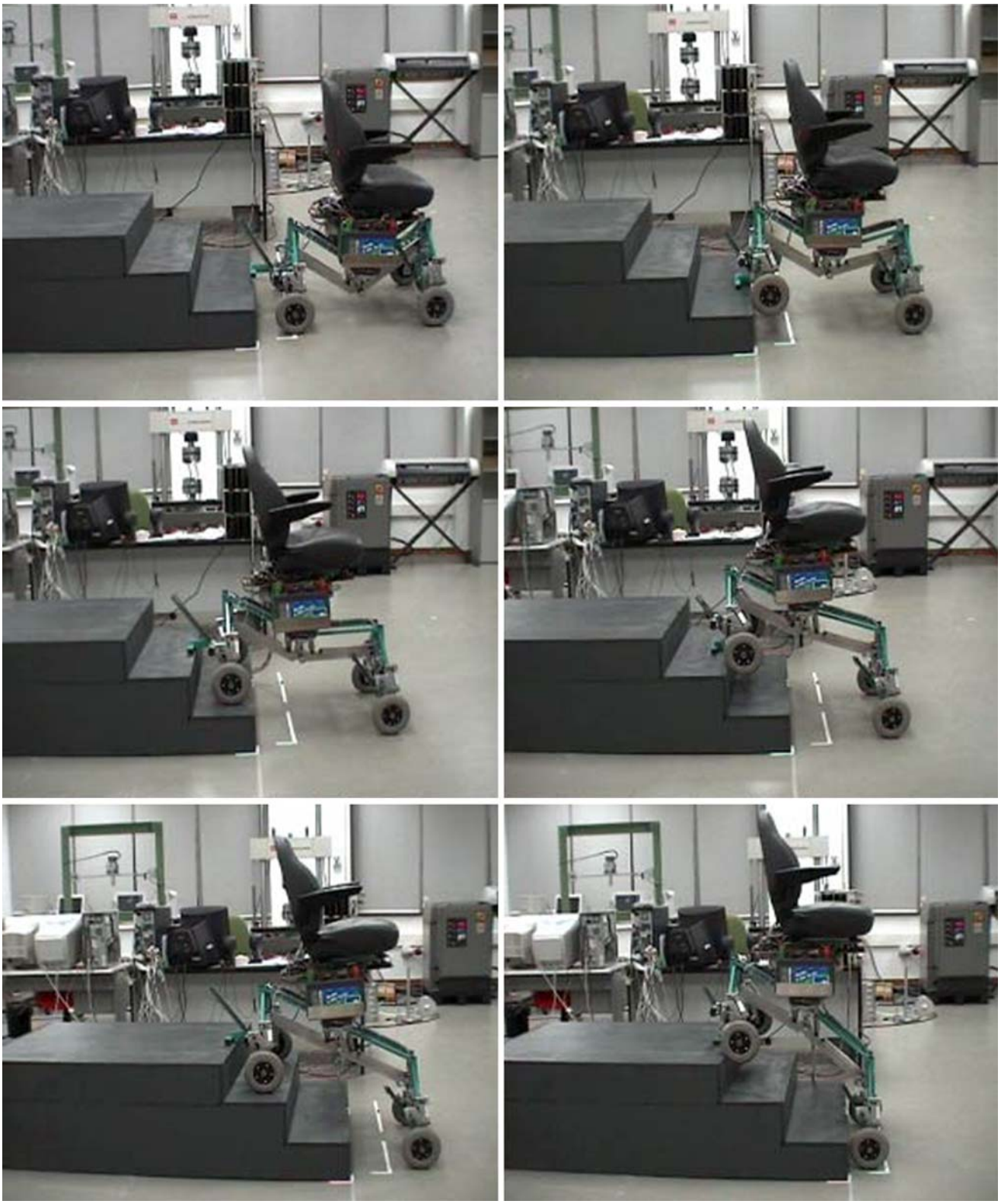

Fig. 22 Sequence of climbing process (Part A)

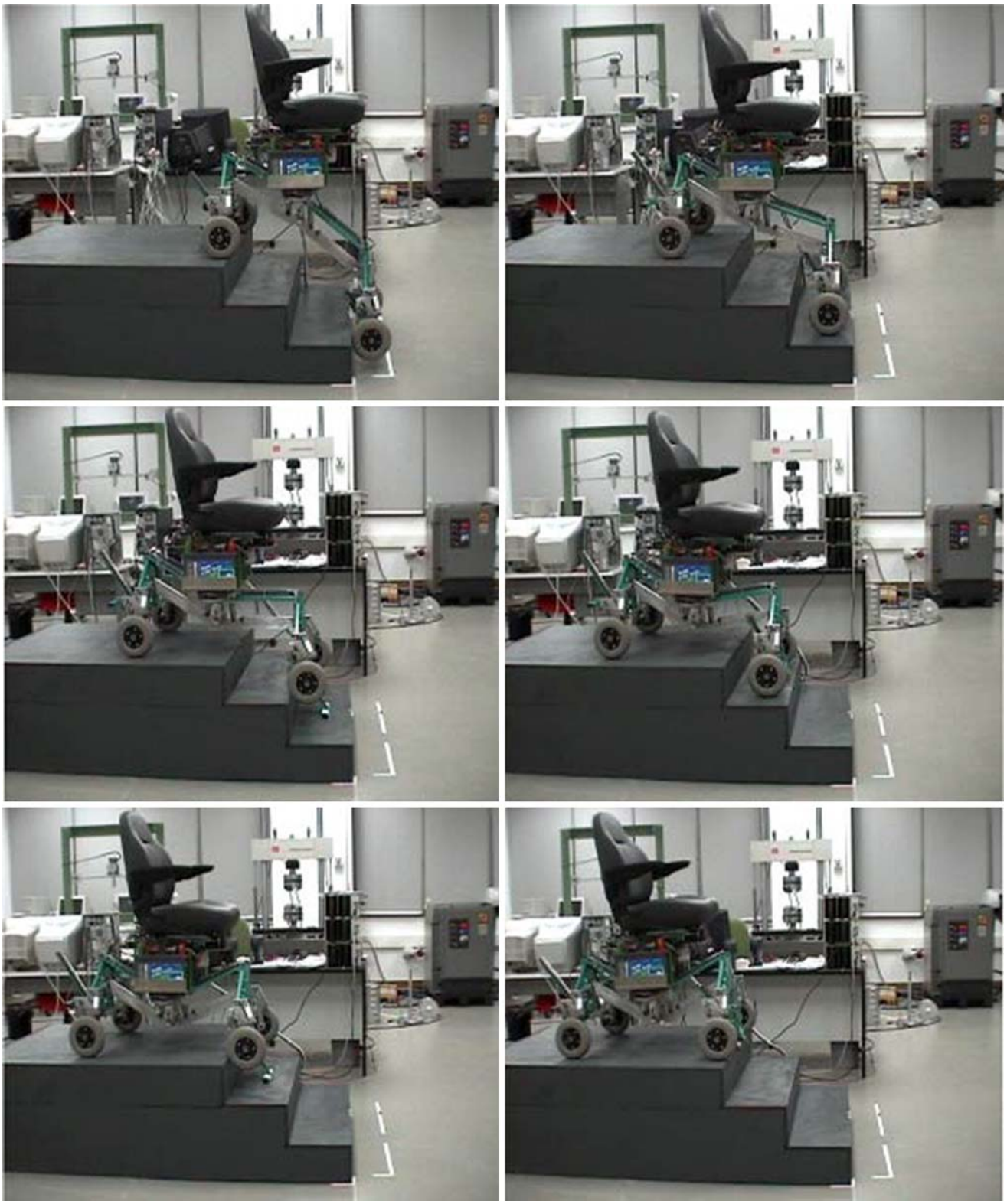

Fig. 23 Sequence of climbing process (Part B)

prototype from dangerous interference. Figure 19B shows that the second actuator (responsible for the angle θ_2) remains constant throughout the trajectory. The responsibility for the climbing process and the maintenance of verticality of the chair is entirely supported by the linear actuator connected to the chair structure in charge of the evolution of θ_1. This finding is in accordance with the theoretical results described in previous sections. Figures 20A and 20B depict the reference and experimental trajectories of the racks, showing the deployment and backward movement of each climbing mechanism when they individually confront obstacles. Figure 21A depicts the reference and the experimental trajectories of the centre of mass as the wheelchair climbs the staircase. The agreement between simulation and experiment is very good as long as the tracking trajectory of the front linear actuator does not surpass the maximum deployment constraint. When the reference trajectory does surpass this limit, there arises a tracking error which remains through the rest of the experiment. Figure 21B shows the evolution of the wheelchair inclination, plotting the reference value, the results obtained by the Optotrack system, and the measurements obtained with the inclinometer. One observes that the two sets of measurements are similar, and that the inclination is close to null. Approximate verticality throughout the trajectory was maintained using open-loop control. Finally, a visual sequence of the climbing process is illustrated in Figs. 22 and 23, showing the different configurations of the wheelchair prototype and the maintenance of verticality of the seat.

6 Conclusions

We have presented a new approach to the design and construction of a step-climbing wheelchair. Its main features are: (a) automatic adaptation to steps of different heights; (b) easy maintenance of the wheelchair's verticality: (c) stair climbing requires less effort from the actuators (only a subset of the actuated degrees of freedom is needed when the trajectory slope of the chair frame is the same as the slope of the racks or the slope of the wheels, depending on the configuration); (d) reduced weight and energy consumption; and (e) wheelchair stability is guaranteed during every moment because its weight is always transferred to horizontal surfaces and the support polygon is always greater than or equal to the support polygon of conventional powered wheelchairs.

The original mechanical problem was split into two subproblems which were solved with separate mechanical devices. The resulting solution has the advantages of very high payload capacity, light weight, and low cost. A methodological approach was described for the appropriate choice of the movement strategy. This choice allows the wheelchair to climb stairs or move along a general smooth profile while maintaining the passenger's comfort and the verticality of the seat by only moving a subset of all the degrees of freedom available in the wheelchair, thereby also reducing the power consumption.

The kinematic model and the climbing strategies were together applied to a wheelchair prototype that we constructed to illustrate the good environment adaptation of our design as it moves over steps of different heights or on a complete staircase. The planned trajectories were consistent and agreed with the experimental results. The smallness of the deviations between the desired and actual trajectories validated the accuracy of our direct and inverse kinematic models for all the chair configurations. The experimental results showed only slight deviations from verticality, and demonstrated that our mechanical design allows the chair to climb stairs with the proposed open-loop control strategy with minimal sensor requirements, while guaranteeing the stability and comfort of the passenger.

In future work, we will complete the control scheme of Fig. 6, including the closed-loop system that uses inclinometer measurements, and the ultrasound sensors that measure the position of the wheels relative to the steps. This will allow faster movements while maintaining the margins of comfort and security for the passenger.

References

Altendofer, R., & Moore, N. (2001). Rhex: A biologically inspired hexadod runner. *Autonomous Robots*, *11*(3), 207–213.

Attali, X., & Pelisse, F. (2001). Looking back on the evolution of electric wheelchairs. *Medical Engineering & Physics*, *23*(10), 735–743.

Cooper, R. A., O'Connor, T. J., Gonzalez, J. P., Boninger, M. L., & Rentschler, A. (1999). Augmentation of the 100 kg ISO wheelchair test dummy to accommodate higher mass: a technical note. *Journal of Rehabilitation Research and Development*, *36*(1), 48–54.

Ding, D., Cooper, R. A., Terashima, S., Yang, Y. S., & Cooper, R. (2004). A study on the balance function of the iBOT transporter. In *Proceedings of the RESNA 2004 annual conference*, Orlando, FL.

Gonzalez, A., Morales, R., Feliu, V., & Pintado, P. (2007). Improving the mechanical design of a new staircase climbing wheelchair. *Industrial Robot: An International Journal*, *34*(2), 110–115.

Gough, V. E., & Whitehall, S. G. (1962). Universal tyre test machine. In *Proceedings of the FISITA 9th international technical congress*, pp. 117–137, May 1962.

Grand, C., Benamar, F., Plumet, F., & Bidaud, P. (2004). Stability and traction optimized of a reconfigurable wheel-legged robot. *The International Journal of Robotics Research*, *23*(10–11), 1041–1058.

Guccione, S., & Muscato, G. (2003). The wheeleg robot. *Robotics and Automation Magazine, IEEE*, *10*(4), 33–43. ISSN: 1070-9932.

Hanavan, E. P. (1964). A mathematical model of the human body. Wright-Patterson Air Force Base, OH, AMRL-TR-64-102, 1964.

Hirose, S. (1984). A study of design and control of a quadruped walking vehicle. *The International Journal Robotics Research*, *3*(2), 113–133.

Hirose, S., & Takeuchi, H. (1996). Study on roller-walk (basic characteristics and its control). In *Proceedings of the IEEE international conference on robotics and automation* (pp. 3265–3270).

Jones, M. L., & Sanford, J. A. (1996). People with mobility impairment in the United States today and in 2010. *Assistive Technology*, *8*(1), 43–53.

Kamen, D. L., Ambrogi, R. R., Heinzmann, J. D., Heinzmann, R. K., Herr, D., & Morrel, J. B. (2002). Control of a balancing personal vehicle, U.S. Patent 6 443 250, Sept. 3, 2002.

Kwon, Y. H. (2001). Experimental simulation of an airborne movement: applicability of the body segment parameter estimation methods. *Journal of Applied Biomechanics*, *17*(3), 232–240.

Lawn, M. J., & Ishimatzu, T. (2003). Modeling of a stair-climbing wheelchair mechanism with high single-step capability. *IEEE Transaction on Neural Systems and Rehabilitation Research, 11*(3).

Miller, D., & Slack, M. (1995). Design and testing of a low-cost robotic wheelchair prototype. *Autonomous Robots*, *2*(1), 77–88.

Morales, R., Feliu, V., Gonzalez, A., & Pintado, P. (2006a). Coordinated motion of a new staircase climbing wheelchair with increased passenger comfort. In *Proceedings of the IEEE international conference on robotics and automation*, pp. 3395–4001.

Morales, R., Feliu, V., Gonzalez, A., & Pintado, P. (2006b). Kinematic model of a new staircase climbing wheelchair and its experimental validation. *The International Journal on Robotics Research*, *25*(9), 825–841.

Sunwa CO. Ltd. Sunwa Stair-Ship TRE-52. Sendagaya, Shiuya-ku, Tokyo Japan. www.sunwa-jp.co.jp.

Stewart, D. A platform with six degrees of freedom. In *Proceedings of the IMechE*, Vol. 180, Pt. 1, No. 15, pp. 371–385, 1965–1966.

Wellman, P., Krovi, V., Kumar, V., & Harwin, W. (1995). Design of a wheelchair with legs for people with motor disabilities. *IEEE Transactions on Rehabilitation Engineering*, *3*(4), 343–353. ISSN: 1063-6528.

Wiesspeiner, G., & Windischbacher, E. (1995). Distributed intelligence to control a stair-climbing wheelchair. IEEE-EMBC and CMBEC. Theme 5: Neuromuscular Systems/Biomechanics.

Woods, B., & Watson, N. (2003). A short history of powered wheelchairs. *Assistive Technology*, *15*(2), 164–180.

R. Morales was born in Spain in 1977. He received his B.S. degree in industrial engineering and his Ph.D. degree from the University of Castilla-La Mancha, Spain in 2002 and 2006, respectively.
He is Assistant Professor of the School of Industrial Engineering, University of Castilla-La Mancha, Albacete, Spain (2002-present). His research interest include design, development and control of industrial robots and also in special robotics systems.
He is author and/or co-author of several papers in refereed professional journals and international conference proceedings.

A. Gonzalez was born in Spain 1969. She received the degree as mechanical engineer at the University of Seville. At the University of Castilla-La Mancha he received the Ph.D. in Industrial Engineering in 2006.
Since 2002 he is Assistant Professor for Mechanics of Machinery and Mechanisms at the University of Cassino. In 2006 he was visiting scholar at the Laboratory of Robotics and Mechatronics, Department of Mechanical Engineering, University of Cassino, Italy. His research interests cover aspects of Mechanics of Robots, Compliant Actuators, and Obstacle-Climbing Vehicles. Specific subjects of his interest is Staircase-Climbing Wheelchairs.
He is author and/or co-author of several papers that have been published in Proceedings of National and International Conferences or in Journals.

V. Feliu (M'88) received his M.S. degree (with honors) in industrial engineering and his Ph.D. degree from the Polytechnical University of Madrid, Spain in 1979 and 1982, respectively.
He was with the Electrical Engineering Departmen, Universidad Nacional de Educación a Distancia, Spain, from 1980 to 1994. He reached the position of Full Professor in 1990 and was Head of the Department from 1991 to 1994. He is Dean of the School of Industrial Engineering, Universidad de Castilla-La Mancha, Spain, since 1994. He is also with E.T.S.I. Industriales, Ciudad Real, Spain. He was a Fulbright Scholar, from 1987 to 1989, at the Robotics Institute, Carnegie Mellon University, Pittsburgh, PA. His research interests include multivariable and digital control systems, and kinematic and dynamic control of rigid and flexible robots. He was written more than 80 technical papers in related areas.
Dr. Feliu is a member of IFAC, ACM and IEEE

P. Pintado graduated as a Mechanical Engineer from the University of Seville (Spain) in 1986 and obtained his Ph.D. from the same university in 1989. He was a Fulbright Fellow in the Virginia Polytechnic Institute during two academic years (1989–1991). He has been Associate Professor with the University of Seville (1991–1998), and he is currently a Full Professor of Mechanical Engineering at the University of Castilla La Mancha (Spain).
His research interests lie along two lines: vibrations and mechanism design. With respect to vibrations he works on road damage caused by heavy vehicle suspensions, active control of pneumatic suspensions, and diagnosis of machinery. With respect to mechanism design he works on the design of staircase-climbing wheelchairs.
He has published forty articles and two books, is author of two patents in Spain, and one commercial computer application. He has worked as consultant for private enterprises in many occasions.